A finite element simulation study on the superficial collagen fibril network of knee cartilage under cyclic loading

Effects of fibril crosslink densities

Komala, Ivan; Chen, Yu Ting; Chen, Ying Chun; Yeh, Chih Ching; Lu, Tung Wu

DOI
10.1016/j.jmbbm.2025.107100

Publication date
2025

Document Version
Final published version

Published in
Journal of the mechanical behavior of biomedical materials

Journal of the Mechanical Behavior of Biomedical Materials 170 (2025) 107100

Contents lists available at ScienceDirect

Journal of the Mechanical Behavior of Biomedical Materials

journal homepage: www.elsevier.com/locate/jmbbm

A finite element simulation study on the superficial collagen fibril network of knee cartilage under cyclic loading: Effects of fibril crosslink densities

Ivan Komala [a,b], Yu-Ting Chen [a], Ying-Chun Chen [a,c], Chih-Ching Yeh [a], Tung-Wu Lu [a,d,e,*]

[a] Department of Biomedical Engineering, National Taiwan University, Taiwan, ROC
[b] Department of Aerospace Structure & Materials, Delft University of Technology, the Netherlands
[c] Department of Mechanical Engineering, National Taiwan University of Science and Technology, Taiwan, ROC
[d] Department of Orthopaedic Surgery, School of Medicine, National Taiwan University, Taiwan, ROC
[e] Health Science and Wellness Research Center, National Taiwan University, Taipei, Taiwan, ROC

ARTICLE INFO

Keywords:
Collagen fibril network
Articular cartilage
Finite element analysis
Computational model
Collagen stiffening

ABSTRACT

Collagen, the most abundant protein in the human body, plays a pivotal role in the functioning of tissues such as cartilage of synovial joints. Mathematical modeling enables the more detailed study of the physical behavior of the network under load bearing. In this study, we aimed to develop a microscopic finite element (FE) modeling approach for the study of the stresses and strains of the collagen fibrils of cartilage under mechanical loading. This new approach enabled the two-dimensional modeling of a series of collagen meshwork at the microscopic level based on typical superficial collagen fibril structures of the articular cartilage. A collagen fibril network, a microscopic structure composed of 24 collagen fibrils, was designed to mimic the typical configuration found in the surface layer of cartilage. Twenty networks were developed, each representing one of three distinct crosslink density levels: high, medium, and low. This setup enabled us to investigate the effects of varying fibril connectivity on the network's morphology and its stress and strain responses under continuous biaxial tensile forces and cyclic loading, simulating the contact forces experienced by knee cartilage during walking. It was found that highly-crosslinked meshwork had greater stiffness than lower-crosslinked meshwork but with higher fibril strain under constant load, and that both the collagen meshwork and individual fibrils became stiffer with reduced deformation after several cycles. The current FE modeling approach provides new insights into the structure-function relationships of the collagen-like meshwork, with a specific focus on the unique role of fibril connectivity under mechanical loads. The current results suggest that collagen stiffening after several cyclic loading may lead to the embrittlement of collagen fibrils, altering the mechanical behavior of the cartilage. This study provides further evidence of the importance of the interfibrillar morphology of collagen meshwork in the mechanical behavior of cartilage. The current model illustrates the functional behavior of the collagen network and can be integrated into more comprehensive multiscale cartilage models that include additional components such as water and proteoglycans, thereby enabling a more complete representation of cartilage mechanics. Future research may utilize this collagen-centric model within broader, multi-phase frameworks to examine interactions between the collagen structure, fluids, and the proteoglycan network. These insights into fibril crosslink density-dependent mechanics may help elucidate early micro-mechanical changes occurring during osteoarthritis progression.

1. Introduction

Articular cartilage in synovial joints is a remarkable connective tissue that facilitates smooth motion between joint surfaces while withstanding compressive loads that can reach several times the body's weight during walking or running. This relies on very complex mechanical interactions between components of its hierarchical structure of proteoglycans, water, and type II collagen (Athanasiou et al., 2013). Among the components, collagen fibrils in knee cartilage resist tensile deformation during compressive loading, acting as passive stabilizers

* Corresponding author. Department of Biomedical Engineering, National Taiwan University, Taipei, Taiwan, ROC.
E-mail address: twlu@ntu.edu.tw (T.-W. Lu).

https://doi.org/10.1016/j.jmbbm.2025.107100
Received 1 September 2024; Received in revised form 3 June 2025; Accepted 8 June 2025
Available online 14 June 2025

rather than transmitters of active tensile forces, while the cartilage itself is subjected to high compressive dynamic loads during activities of daily living such as walking or running (Mononen et al., 2012; Saarakkala et al., 2010). Across the depth of the articular cartilage, fibrils at the superficial zone mainly protect the tissue from excessive strain tangential to the articular surface. Conversely, collagen fibrils in the deep zone predominantly withstand compressive stresses due to their vertical orientation. Any tensile stress they encounter is minimal and results from counteracting shear deformations, rather than conveying significant tensile forces perpendicular to the subchondral bone surface (Shirazi et al., 2008). Disruption or loosening of the collagen fibril network at the superficial zone has been suggested as a sign of osteoarthritis (OA) (Guilak et al., 1994; Orford et al., 1983). A study has found that collagen fibrils become stiffer with aging (Verzijl et al., 2002) and after repetitive tension tests (Liu et al., 2018). Embrittlement of the collagen fibril is considered as the initiation of OA (Chen and Brown, 2020). Alterations of the ultrastructure or the changes in the material properties of the collagen fibril network may change the loading mechanism of the cartilage and possibly damage the articular cartilage (Guilak et al., 1994; Huber et al., 2000). Since cartilage experiences different cyclic loading such as walking or running during daily life, with its limited healing ability, it is important to understand the role of the collagen fibrils network and the effects of repetitive loadings and arrangement of the collagen fibrils on the mechanical properties of the collagen fibrils network. A previous study on collagen mechanics (Buehler, 2006) demonstrated that nanoscale architecture and crosslinking within collagen fibrils significantly impact the tissue's macroscopic mechanical properties. Depalle et al. (2015) highlighted that both crosslink type and density critically influence fibril stiffness and failure mechanics, underscoring the importance of crosslinking in collagen's mechanical behavior under stress.

Various modalities such as X-ray and MRI are often used clinically to diagnose OA, but they only detect macroscopic damage and lack sensitivity to early, microscale collagen network changes (Burstein and Gray, 2006; Li et al., 2007; Glover and Mansfield, 2002). Optical microscopy techniques (e.g. polarized light or SHG imaging) can reveal fibril orientation, they do not provide high-resolution, three-dimensional insight into fibril-crosslink interactions under mechanical load (Broom et al., 2001a; Brown et al., 2012, 2014; Chen and Broom, 1998a). Non-invasive spectroscopic methods (e.g. near-infrared reflectance) can correlate cartilage composition and thickness with biomechanical properties (Oberg et al., 2004; Johansson et al., 2011; Afara et al., 2015; Arokoski et al., 1996; Panula et al., 1998), yet still lack the spatial and structural resolution to capture fibril-crosslink mechanics under load. Advanced optical techniques such as polarized-light microscopy and second-harmonic generation imaging (Wang et al., 2021a; Korhonen et al., 2002) likewise cannot resolve three-dimensional fibril-crosslink interactions under physiological strain.

Computational models are an effective approach for quantitatively examining changes in the shape and mechanical properties of the collagen fibril network under regular ambulation. Early studies, such as those by Mow et al. (1984), focused on interstitial fluid movement within cartilage, laying the foundation for the development of subsequent constitutive equations. The three-phase theory, developed by Lai et al. (1991), explains cartilage swelling and deformation, with broad applications in cartilage mechanics. In recent years, sophisticated constitutive models of articular cartilage have been established to describe the cartilage mechanics at the tissue level (Pierce et al., 2013; Deneweth et al., 2013; Ateshian et al., 2009). Recent trends in cartilage rheology modeling have been highlighted by Zhao et al. (2020), who explored new constitutive models that enhance our understanding of tissue behavior at the microscale. Additionally, Li et al. (2019) and Wang and Sun, 2021b expanded this field by developing multiscale models that link molecular to tissue-level structures, providing insights into cartilage structure-function relationships. The mechanical contributions of the collagen fibrils to the cartilage were considered implicitly in the constitutive models. With such approaches, realistic loading conditions or articular cartilage morphology were difficult to model and the morphological changes of the fibril network could not be identified. Finite element (FE) models, which incorporate established constitutive laws and detailed structural information, enable realistic simulations of cartilage shape and mechanical response within a continuum setting. Studies have shown that FE models accounting for collagen network orientation and viscoelasticity provide valuable insights into cartilage mechanics (Julkunen et al., 2007; Wilson et al., 2004; Pierce et al., 2009). These studies reveal the depth-dependent behavior of cartilage, enhancing our understanding of tissue responses under various loading conditions. To better represent the contributions of the collagen fibrils in the study of the cartilage behavior, a 3D fibril-reinforced poroviscoelastic material model was used in a macroscopic FE model of knee cartilage incorporating depth-dependent mechanical behavior of the collagen network (Wilson et al., 2004; Benninghoff, 1925) and the orientations of the collagen fibrils in the continuum elements (Mononen et al., 2012). Finite element modeling has also been used for micro-structure level modeling of the cartilage in the deep zone as continuum elements incorporating properties of chondrocytes, type II collagen, and proteoglycan (de Andréa et al., 2019). Finite element (FE) models have been instrumental in studying the mechanical behavior of articular cartilage. However, many studies primarily focus on large-scale mechanical responses and often overlook small-scale structural changes in the collagen fibril network. For example, Shirazi et al. (2008) highlighted the mechanical roles of deep vertical and superficial horizontal fibrils under compression, while Wilson et al. (2004) developed a poroviscoelastic model to examine local stress and strain within the fibril network. Although these models address larger or localized stresses, they frequently overlook detailed changes in fibril connectivity and arrangement under repeated loading. Our approach aims to address this gap by focusing on structural changes at the fibril level during continuous loading. Chen et al. proposed a 2D microscopic model of the collagen network to explore the relationship between the fibril interactions in the collagen network and the consequent mechanical performance and restructuring under load (Chen et al., 2017). However, the material properties of the collagen fibrils were assumed elastic, so the morphological and mechanical responses of the collagen fibrils to external loads and the loading rates could not be studied. To the best of the authors' knowledge, although several studies have quantitatively analyzed the mechanical properties and certain aspects of the structural arrangement of the collagen fibril network (Brown et al., 2012; Stein et al., 2008), comprehensive assessments that integrate detailed morphological changes with mechanical responses under specific conditions remain limited.

The purposes of the current study were to develop a two-dimensional microscopic FE model of collagen meshwork based on typical collagen fibril structures of the superficial zone of knee articular cartilage and to study the effects of fibril crosslinking densities on the stresses and strains of the collagen fibrils under loading/recovery and cyclic loading/unloading tests. It was hypothesized that compared to lower crosslink densities collagen fibril networks with higher densities would deform less but with increased local fibril strains and stresses, especially under cyclic loadings.

2. Methods

2.1. FE mesh for collagen fibril network models

For the study of the mechanics of the collagen fibril networks of the superficial zone of knee articular cartilage using two-dimensional microscopic FE modeling, the morphological collagen fibril network was first constructed according to electron micrographs of the knee articular cartilage surface (Teshima et al., 1995; Broom et al., 2001b) and the microstructure modeled as a node-spring network (Chen et al., 2017). In the current collagen fibril network model, 30 fibrils with

lengths of approximately 24 μm were initially placed in parallel to each other at a distance of 1 μm, giving a rectangular shape of approximately 24 by 30 μm (Fig. 1). Each fibril consisted of a series of 50 nm diameter (Hwang et al., 1992; Tang et al., 2014) wires connected by 25 nodal points (Fig. 1). To generate different collagen network configurations, the nodes were randomly displaced in the horizontal direction for less than 1 μm. Two adjacent fibrils were then connected by crosslinks between nodes with distances less than proximity thresholds of 0.6 μm, 0.8 μm, and 0.9 μm corresponding to low, medium and high crosslink densities, respectively (Fig. 1). Interfibrillar lengths in this study were derived from literature-based structural ranges (Broom et al., 2001b), rather than direct experimental measurement, to emphasize the collagen matrix's mechanical properties. The chosen 1 μm value is representative of this range and ensures that our model reliably captures the behavior of the fibril network under stress. High crosslink densities were considered representative for collagen fibril networks in healthy cartilage and taken as controls in the current study. With the low crosslink density, the collagen fibril network reconstructed a similar network structure found in cartilage specimens from early OA (Chen and Broom, 1998b). The network generation procedure was implemented in MATLAB (R2019a, The Mathworks Inc., USA). The geometrical model of the fibril network was then imported to the ABAQUS v6.14 (Dassault Systèmes Simula Corp., Providence, USA), and each wire and crosslink was modeled by 5 truss elements (T2D2) according to convergence tests with a 1 % tolerance. In the current study, twenty models were generated for each of low-, medium-, and high-density crosslinked collagen networks, consisting of approximately 2300, 2600, and 2800 elements, respectively.

2.2. Material properties of the collagen fibrils and crosslinks

In the current FE modeling, the collagen fibril was modeled as visco-hyperelastic materials. The hyperelastic properties were described using the 3rd order Ogden strain density formula (Ogden, 1997) as follows.

$$U = \sum_{i=1}^{N} \frac{2\mu_i}{\alpha_i^2} \left(\lambda_1^{-\alpha_i} + \lambda_2^{-\alpha_i} + \lambda_3^{-\alpha_i} - 3\right), \quad (1)$$

where U is the strain density, μ_i and α_i are material parameters and λ is the principal stretch with assumptions of incompressibility. The material parameters μ_i and α_i were obtained by fitting the experimental data of a single collagen fibril from van der Rijt et al. (van der et al., 2006) to Eq. (1) (Table 1). The viscoelastic material properties were described by the Prony series as follows (Heidari, 2011):

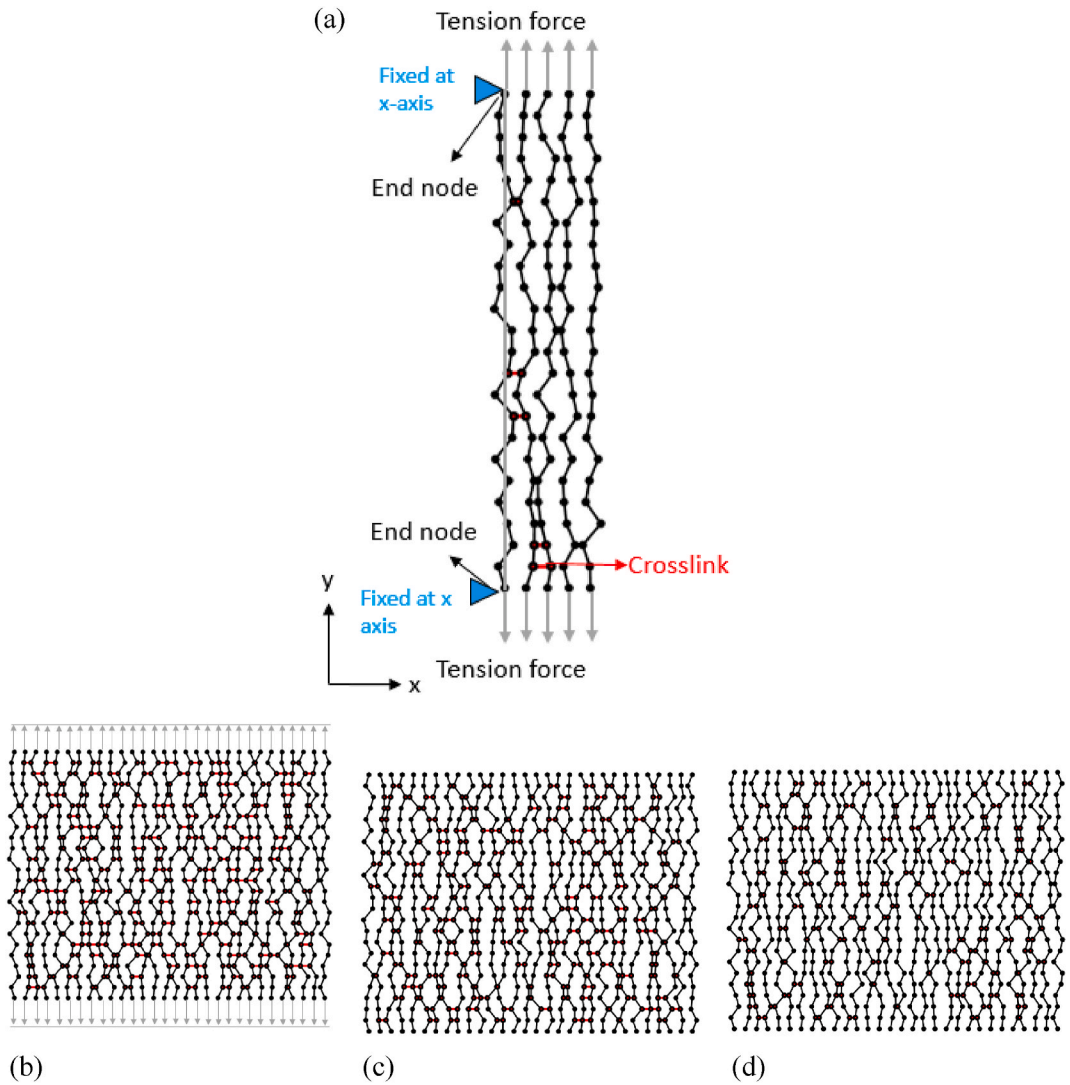

Fig. 1. Typical collagen fibril networks (a) with randomly generated nodal positions connecting the collagen fibrils (black) and with crosslinks (red) for (b) low, (c) medium and (d) high crosslink densities created according to inter-nodal horizontal distance thresholds of 0.6 μm, 0.8 μm and 0.9 μm, respectively.

Table 1
Material parameters for collagen fibrils as visco-hyperelastic materials.

	Hyperelastic parameters		Prony series parameters	
i	μ_i	α_i	g_i	τ_i
1	−88006.8831	1.9983	0.7284	5.7227
2	57753.4773	3.9983	−0.54052	7.4702
3	30331.4509	−2.0016	0.18212	52.413

$$G(t) = G_0 - \sum_{i=1}^{N} G_i \left[1 - e^{\left(-t/\tau_i\right)}\right], \tag{2}$$

where $G(t)$ is the tensile modulus at time t, G_0 is the initial tensile modulus, and τ_i is the relaxation time. The relation between $G(t)$ and G_0 can be expressed as the dimensionless tensile modulus (g_R):

$$g_R(t) = \frac{G(t)}{G_0} \tag{3}$$

Therefore,

$$g_R(t) = 1 - \sum_{i=1}^{N} g_i \left[1 - e^{\left(-t/\tau_i\right)}\right] \tag{4}$$

The viscoelastic parameters τ_i and g_i were obtained by fitting experimental data on articular cartilage (Woo et al., 2006) to Eq. (4) (Table 1). Because no direct viscoelastic tests on isolated type II collagen fibrils are yet available, we provisionally adopted tissue-level relaxation data from knee ligaments (predominantly type I collagen) as a surrogate. The material properties of the crosslinks were assumed to be the same as those of the collagen fibrils used in this study due to a lack of available information in the literature.

2.3. Loading/recovery tests

The FE model of the collagen fibril network was first used to study the viscoelastic responses of individual fibrils during the loading and recovery process of a uniformly distributed tensile force of 12 μN (Chen et al., 2017). Since the current model was developed to simulate the fibril network of the superficial zone of the articular cartilage, where the collagen fibrils were mainly under tensile loading, the uniformly distributed tension was applied at each end node of all the fibrils to give longitudinal stretch mimicking the loading conditions in the cartilage (Fig. 1). The end nodes were constrained in the transverse direction to approximate the lateral support of the surrounding matrix and prevent non-physiological buckling under axial tension. Pilot simulations without this constraint exhibited excessive lateral deflection and convergence issues, which are not observed in micromechanical tensile tests of collagen fibrils (Thambyah and Broom, 2006; Tang et al., 2010). During the loading/recovery simulations, the fibril network was stretched by the uniformly distributed tension for 10 s and then released. The dynamic changes of the stress and strain distributions were observed throughout the 10s loading process and for 110 s after the force was released. We also performed a pilot simulation that contained 100 s of loading and 100 s of recovery and found that the strain rate was the biggest immediately after loading, reduced dramatically to around 0.02 s^{-1} at 10 s and remained more or less unchanged after 10 s. The duration of 100 s for recovery was determined as the time when the strains of all the fibrils were less than 0.01. Under the 10 s/100 s loading regime, the loading/recovery simulations were performed for each of the sixty models of fibril networks. The dynamic simulations were executed using automatic time increments with an initial value of 0.1s and adjusted within the range of 0.00001s–1s per frame defined by the FE software. The strains and stresses of all the fibrils were averaged to obtain the average fibril strains and stresses at 10s and 100s and the time at 30 %, 60 % and 90 % of recovery during the unloading/recovery phase for each model. The bulk strains for the whole fibril network at the same instants were also calculated as the total displacements of the end nodes divided by the original lengths of the fibril network.

2.4. Cyclic loading/unloading tests

The viscoelastic responses of individual fibrils of the collagen fibril network under cyclic loading/unloading conditions were also simulated using the FE model to indicate the mechanical responses during repetitive activities of daily living such as walking. Each model was subject to 25 cycles of 1 s/1 s loading/unloading of a uniformly distributed tensile force of 12 μN (i.e., 2Hz). Dynamic simulations were performed for each of the sixty models of fibril networks. The average fibril strains and stresses and the bulk strains were obtained throughout the whole period of the test for each of the models. The peak values of the average strains and stresses and bulk strains were obtained for each cycle for each model. The stiffness values were also calculated as the gradients of the average stress-strain curves, and the average stiffness for each cycle and each model was obtained. The peak average strains and stresses were also averaged across all cycles to get the cycle-mean strains and stresses for each model.

2.5. Statistical analysis

For loading/recovery tests, the average fibril strains and stresses and bulk strains and stresses at 10s and 110s and the time at 30 %, 60 % and 90 % of recovery during unloading were compared between low, medium and high fibril crosslink densities using one-way analysis of variance (ANOVA). If a significant main fibril crosslink density effect was found, a *post hoc* trend analysis was performed to determine the trend of the variable with increasing cross-link densities. The possible relationship between the number of crosslinks and the average fibril strains and bulk strains was tested by using linear regression analysis. For cyclic loading/unloading tests, the average stiffness values for all models were analyzed using two-way ANOVA with a between-group factor (low, medium, high) and a within-group factor (25 cycles). The cycle-mean strains and stresses were compared between low, medium, and high densities using one-way ANOVA. All significance levels were set at $\alpha = 0.05$. SPSS version 20 (SPSS Inc., Chicago, USA) was used for all statistical analysis.

3. Results

3.1. Loading/recovery tests

The fibril strains and stresses increased significantly in a nonhomogeneous fashion within the network under tensile load (Fig. 2). At 10 s during the loading phase, the average fibril strains within a model of high crosslink density ranged from 6.48 % to 6.6 % with a mean value of 6.56 % across all twenty models (Table 2), the higher strains being in the fibrils in the center regions of the network (Fig. 2). The corresponding values for stresses were 64.73, 65.45 and 65.1 MPa, respectively (Table 2). Similar patterns of average fibril strains were also found for models with low and medium crosslink densities (Fig. 3). The mean average fibril strains at 10 s were 6.5 %, 6.545 %, and 6.562 %, for low-, medium-, and high-density models, respectively, increasing linearly with increasing crosslink densities ($p < 0.05$; Table 2). The mean bulk strains at 10 s across models with low-, medium-, and high-density were 13.37 %, 12.69 %, and 12.434 %, respectively, showing a significant linear decreasing trend ($p < 0.05$; Table 2). At 100 s after the release of load, all the models almost returned to the unloaded state with the average fibril strains reduced by approximately 99.7 % of the maximum average fibril strains. The average fibril strains were statistically different between low-, medium-, and high-density models, increasing linearly with increasing crosslink densities ($p < 0.05$; Table 2) while the

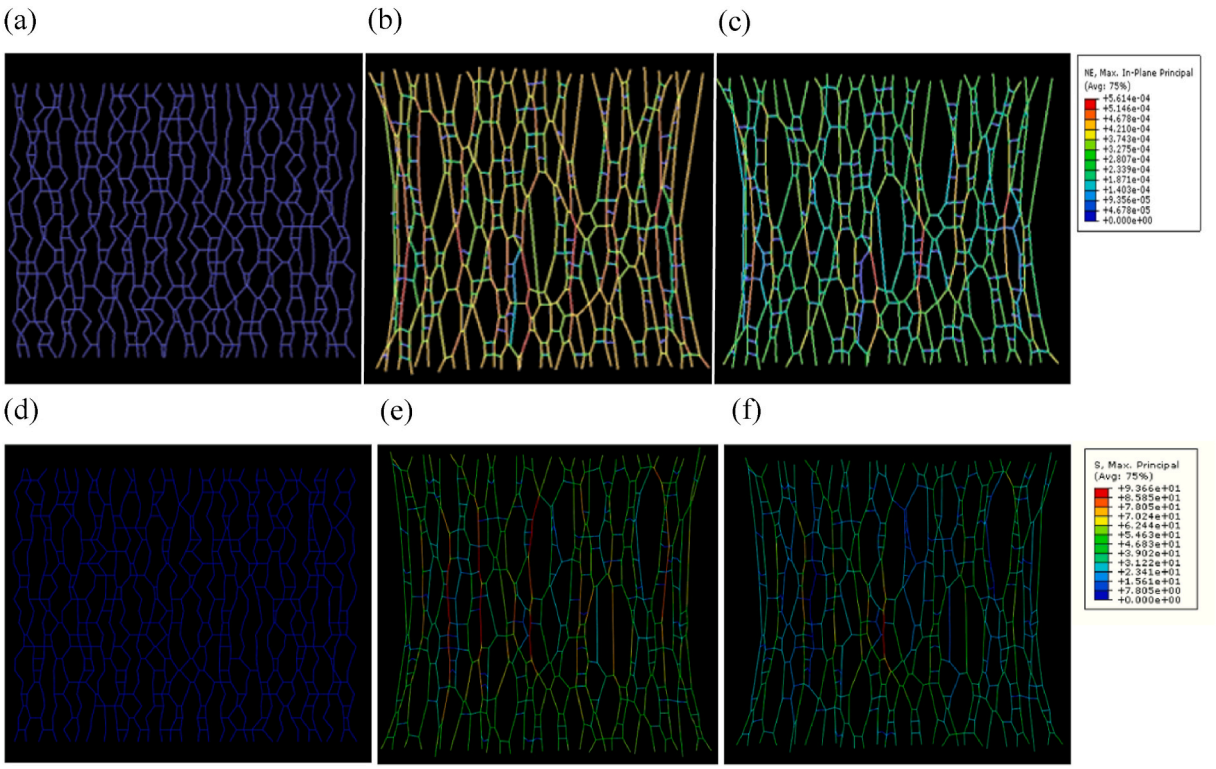

Fig. 2. Maximum principal strain distributions of a typical collagen fibril network with high crosslink density (a) at unloaded condition (b) under a tensile force of 12 μN for 10s, and (c) 120s after the release of the force. The corresponding maximum principal stress distributions are shown in (d–f).

Table 2
Means, standard deviations, minimum and minimum values of the average fibril strains, peak fibril strains, and bulk strains over 10 s during loading phase and recovery rates at 100s after force release for collagen fibril networks with low (n = 20), medium (n = 20) and high (n = 20) crosslink densities during loading/recovery with a tensile force of 12 μN.

	Crosslink density	Mean	Standard Deviation	P_{LH}	P_{LM}	P_{MH}	Trend
Loading Phase (0–10 s)							
Average Fibril Strain (%)	Low	6.50	0.05	**0.0001***	**0.0045***	0.414	↑
	Medium	6.55	0.04				
	High	6.56	0.03				
Peak Fibril Strain (%)	Low	8.11	0.31	0.975	0.998	0.988	↓
	Medium	8.10	0.24				
	High	8.09	0.21				
Bulk Strain (%)	Low	13.38	0.34	**0.0001***	**0.0001***	0.043	↓
	Medium	12.73	0.37				
	High	12.46	0.32				
Unloading/recovery phase (100 s)							
Fibril Recovery (%)	Low	0.03	0.02	0.997	0.997	1.000	–
	Medium	0.03	0.02				
	High	0.03	0.02				
Peak Fibril Recovery (%)	Low	4.83	0.44	0.801	0.805	1.000	↓
	Medium	4.72	0.41				
	High	4.72	0.34				
Bulk Recovery (%)	Low	6.01	0.28	**0.0001***	**0.0001***	**0.0022***	↓
	Medium	5.16	0.41				
	High	4.78	0.32				

P_{LH}, P_{LM}, P_{MH} are p-values for low vs. high, low vs. medium, and medium vs. high density comparisons, respectively. * indicates significant difference ($p < 0.05$); ↑ indicates a linearly increasing trend with increasing density and ↓ indicates a linearly decreasing trend ($P_d < 0.05$).

bulk strains showed a statistically linear increasing trend ($p < 0.05$; Table 2).

3.2. Cyclic loading/unloading tests

The high density models showed a peak average fibril strain of approximately 6.45 %, a peak average stress of 65.9 MPa, a peak bulk strain of 12.92 % and a peak average bulk strain of 12.32 % at the end of the 1 s loading phase during the first cycle and the corresponding values for the second cycle were 6.53 % and 66 MPa, 13.07 % and 12.44 %, respectively (Fig. 4). These values increased with increasing cycles, showing a rapid increase over the first 4 cycles and slowing down for the rest of the cycles until reaching the peak values of 6.86 %, 66.1 MPa, 13.59 % and 12.78 %, respectively, after 25 cycles (Fig. 4). The peak

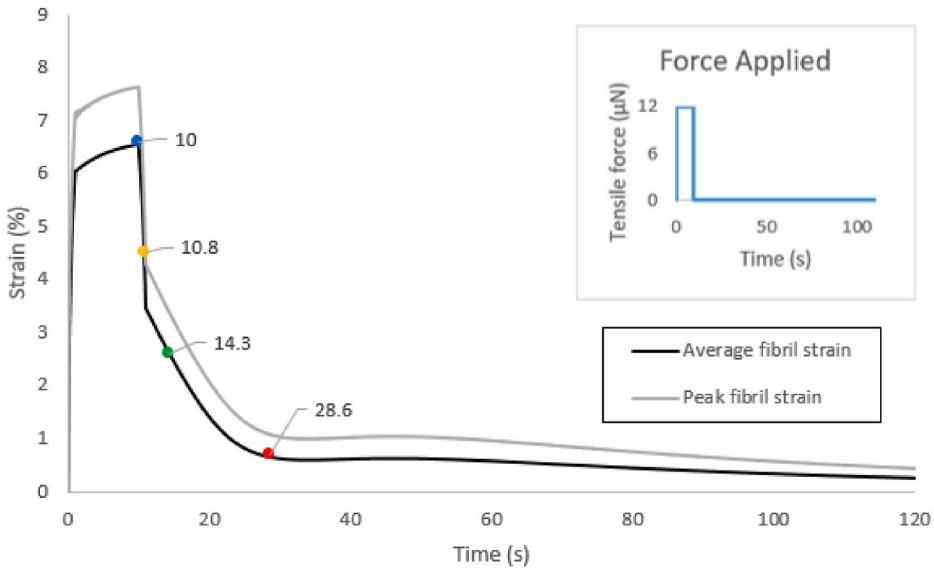

Fig. 3. Average fibril strains (black) and peak fibril strains (grey) over time during the loading/recovery tests with a constant tensile load of 12 μN during the first 10s (loading phase) followed by 100s period after the release of the load (unloading/recovery phase) for models of high crosslink densities, showing the time-dependent strain accumulation during the loading phase and the viscoelastic recovery behavior during the unloading phase. The times are also indicated at 10s (blue dot), 30 % of recovery (orange dot), 60 % of recovery (green dot) and 90 % of recovery (red dot). Similar curves were also found for models of low and medium crosslink densities.

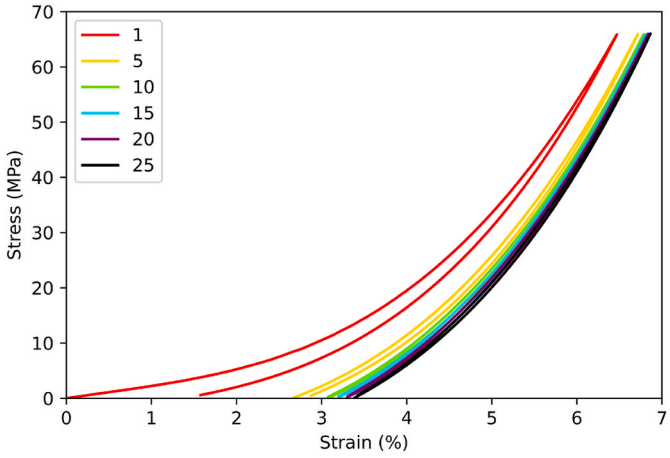

Fig. 4. Stress-strain curves of the collagen fibril network of high density during the cyclic tension test. The stress-strain curves shifted to the right and the slope was steeper as the number of cycles increased.

stiffness of the fibril networks of high densities increased with increasing number of cycles, indicating a stiffening phenomenon (Fig. 4). The increase of the peak average strains and peak average bulk strains slowed down after about 7 cycles for all models (Fig. 5). Similar phenomena were also found for models with medium and low densities except that the average fibril strains and stress and bulk strain values for models with low densities were significantly smaller than those of the models with medium and high densities, which were of no significant differences (Fig. 5).

4. Discussion

The current study aimed to develop a two-dimensional microscopic FE model of collagen meshwork based on typical collagen fibril structures of the superficial zone of knee articular cartilage and using this model to study the effects of fibril crosslinking densities on the stresses and strains of the collagen fibrils of cartilage under loading and unloading tests and under repetitive physiological loadings during walking. The results support the hypothesis that collagen fibril networks with higher densities would deform less but with increased local fibril strains and stresses. These results suggest that fibril crosslinking densities helped increase the stiffness of the collagen fibril networks as a structure but with an increased risk of early fibril failure and that repetitive loading may stiffen the collagen structures leading to embrittlement.

A 2-D finite element model of the collagen fibril network was developed to investigate the effect of the interconnectivity of the structure and mechanical properties of the fibrils under tensile loads. By incorporating Prony-series visco-hyperelastic fibril properties calibrated from single-fibril and tissue-level relaxation tests (van der et al., 2006; Woo et al., 2006), this model reproduces experimentally observed creep and recovery behaviors at the fibril-network scale and quantifies how crosslink density modulates these time-dependent responses, aspects not addressed in the purely elastic spring-node framework of Chen and Brown. (2020). In the present simulations, morphological changes are visualized via contour plots of maximum principal strain (Fig. 2a–c), and the corresponding contour plots of maximum principal stress (Fig. 2d–f) provide a basis for future estimation of fibril tensile failure likelihood. The results obtained from the current two-dimensional simulations revealed the mechanical responses of the fibril network in the superficial zone of the articular cartilage and the effects of crosslink densities on the mechanical responses. Previous studies have shown that the architecture of the collagen fibril network has a significant influence on the network's ability in resisting load (Bullough and Goodfellow, 1968; Goodwin et al., 2004; Leo et al., 2004; Böttcher et al., 2009). Different network architectures may lead to different values or distributions of the fibril and bulk stresses and strains. To accommodate such variabilities twenty network architectures were generated randomly in the current study, based on a previously suggested network morphology formed from the fibril architecture of the articular cartilage observed with transmission electron microscopy (Eyre, 2001). For the networks in the middle zone when the network is subjected to the tri-directional loadings, a 3D model would be needed.

During loading and recovery tensile tests, the current fibril network models exhibited time-dependent strain accumulation during the 10 s loading phase and viscoelastic recovery during the 110 s unloading/

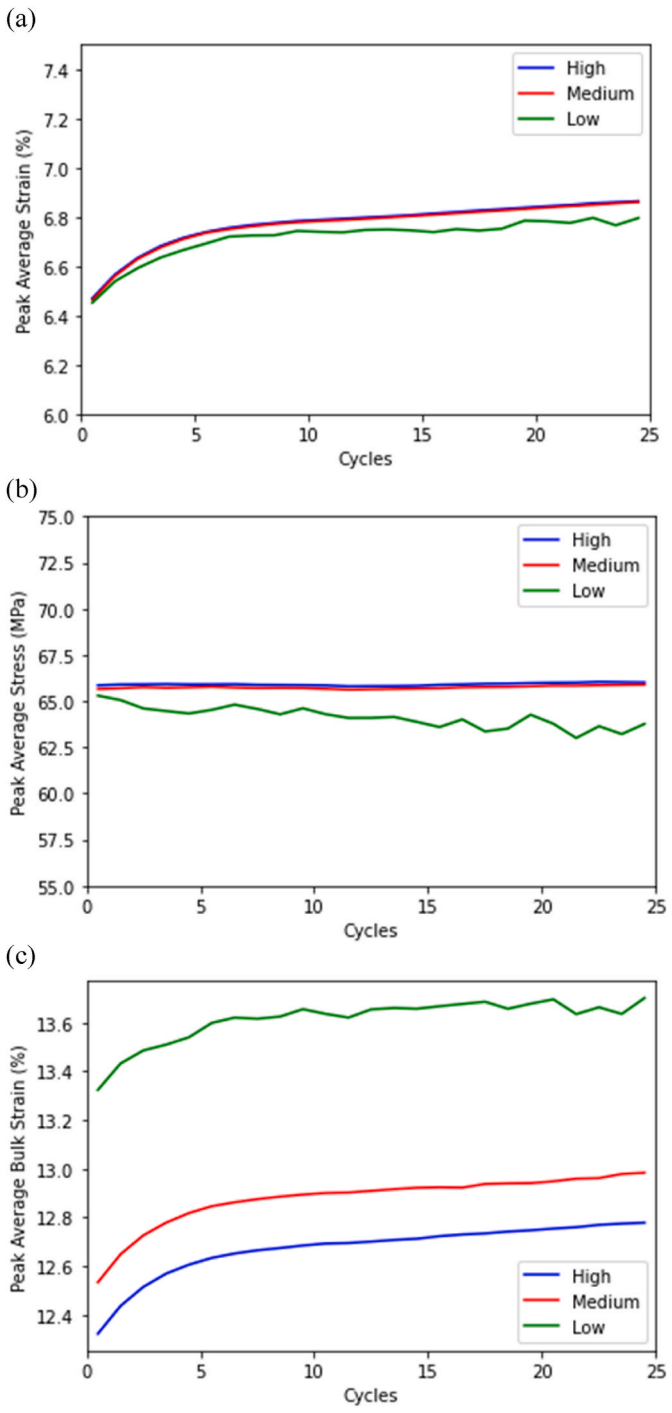

Figure 5. The peak average fibril strains and stresses and the peak average bulk strains of the collagen fibril networks (20 networks for each of the low, medium and high density models) against the number of cycles during the cyclic loading test. (a) The peak average fibril strain increased over time before it reached a steady state (<0.005 % difference/cycle) approximately after 10 cycles. After 20 cycles, the fibril strain plateaued with approximately 6.8 % strain for high and medium crosslink density models. (b) The peak average fibril stress increased by approximately 0.3 % during the first few cycles and then became steady at 66 MPa for high and medium crosslink density models. No obvious differences between high and medium density models were found but the low density models showed peak average fibril strains and stress significantly lower than the other two densities. (c) The peak average bulk strain showed a similar trend to the peak average fibril strain. The high crosslink density models have a lower value compared to the medium and low density models with 12.78 %, 12.98 and 13.702, respectively at the 25th cycle.

recovery phase (Fig. 3), in agreement with micromechanical stress-relaxation tests on individual collagen fibrils (van der et al., 2006) and tissue-level stress-relaxation behavior (Woo et al., 2006), as well as cyclic stiffening observed experimentally in collagen networks (Susilo et al., 2016a). Although the strain-time curves appear nonlinear, this is a typical feature of time-dependent responses in linear viscoelastic materials. These loops arise from linear viscoelastic behavior and should not be interpreted as evidence of true non-linear viscoelasticity, which requires a nonlinear stress–strain relationship at equilibrium. Upon applying the tensile force, the current fibril network models showed an immediate increase in the strain at the highest strain rate and reaching a plateau after 10 s (Fig. 3). After the release of the tensile force, the strains reduced nonlinearly and returned to less than 0.01 μ after 110 s (Fig. 3). Previous studies have primarily employed elastic or phenomenological descriptions (Deneweth et al., 2013; de Andréa et al., 2019; Chen et al., 2017; Ayyalasomayajula et al., 2019), and did not explicitly model collagen fibril viscoelasticity (Chen and Brown, 2020), limiting their ability to reproduce time-dependent strain accumulation and stress recovery observed experimentally (van der et al., 2006; Yang et al., 2012; Bridgman, 2013). In contrast, our model incorporates microscale fiber architecture and Prony-series visco-hyperelastic properties, enabling reproducible capture of both average and bulk strain changes during loading and unloading.

The crosslink density in the fibril network was found to affect the time-dependent behaviors of the network significantly in response to the loading/unloading of the tensile forces. Increasing the crosslink density increased the fibril strains and also increased resistance to bulk deformation, as indicated by the linear increasing trend for fibril strains and linear decreasing trend for bulk strains with increasing crosslink densities (Table 2). These phenomena were in agreement with the previous experimental results (Susilo et al., 2016b). The bulk strain described the response of the collagen fibril network to the applied loads as one unit. The higher the density in the structure, the stiffer the collagen fibril network was. Therefore, compared to collagen fibril networks with lower crosslink densities, those with higher densities deformed less but with increased local fibril strains and stresses (Table 2), leading to an increased risk of early fibril failure. These phenomena in networks with high crosslink densities revealed the necking behavior of the fibril networks. Necking behavior describes the localized reduction of the cross-sectional area with increased localized strains in the necking area of a specimen under tensile load (Bridgman, 2013). In the current study, the collagen fibril network as a single unit with higher crosslink densities showed lower bulk strain whereas the localized fibril strain increased. Similar behavior was also described in a previous computational study of a fibril network model with high crosslink density for the alveolar wall (Casey et al., 2021). In the current study, it was found that the necking behavior only occurred for networks with high densities (Fig. 2). The crosslink density did not appear to affect the durations for 30 %, 60 % and 90 % of the recovery, with between-density differences of less than 0.1s. Since the structures with different crosslink densities were generated with random distributions, locations, and lengths, the results are considered a better representation of the real conditions of fibril networks in the tangential zone of articular cartilage. This is an advantage over previous studies that used only one or a limited number of models (de Andréa et al., 2019).

Investigations of the mechanical changes of the fibril networks in the cartilage during the progression of knee OA are limited because *in vivo* experimental observations of the mechanical behavior over a long time are difficult if not impossible. Hence, the proposed model and simulation approach provide a useful platform for the study of the effects of various mechanical factors that may affect the progression of OA. In this study, the collagen fibril network model with high-density crosslink distribution was used to simulate knee cartilage in healthy subjects while those with medium-density crosslink were used to simulate early OA and low-density crosslink to simulate the earliest stage of OA. This was comparable to previous reports on the reduction of collagen content in the fibril

network in early knee OA (Saarakkala et al., 2010; Tang et al., 2010; Aigner and Stöve, 2003). The current FE model showed that compared to high-density crosslink structures, low-density crosslink density ones showed more tangled fibrils during unloading, in agreement with experimental observations in softened collagen fibril networks (Chen and Broom, 1998a). The cyclic loading-unloading tests were conducted to see the mechanical responses of collagen fibrils when subject to similar repetitive dynamic loads, such as those during walking. The slopes of the stress-strain curves were increased after a long period of cyclic loading (Fig. 4), suggesting the stiffening of collagen fibrils in the fibril network. These results are in agreement with a previous experimental study showing that the collagen fibrils became stronger and tougher when they were repeatedly stretched (Liu et al., 2018). Previous experimental studies have also found that prolonged intensive activities could cause damage to the collagen fibril network, or even lead to early OA due to the stiffening of collagen fibrils (Dahaghin et al., 2009; Loening et al., 2000; Radin et al., 1984). Further simulations on structures with a wider range of crosslinking numbers under cyclic loading may aid to understand the role of interconnectivity between fibrils and its effect on mechanical behavior.

Apart from cyclic loadings, previous studies also found that increased loading rates were closely correlated to a reduced ability for shock absorption (Cook et al., 1997) and a reduced ability of the muscles to attenuate impulsive loading from the ground. Increased loading rates of the repetitive impulsive ground reaction forces (GRF) and thus the joint contact forces experienced at heel strike correlate closely to the development of a variety of pathological conditions, including knee OA (Mündermann et al., 2005). Further studies may use the current models to identify the relationship between loading rates and the mechanical changes within the fibril network during walking, which may help reveal the mechanisms underlying the progression of osteoarthritic changes within the knee cartilage arising from the repetitive impacts during walking. Further studies may also be extended to the mechanisms of the failure behavior of collagen fibrils by simulating different material properties in the current micromechanical model. Moreover, the current fibril network configuration was based on a previous study, further study using different fibril structures such as *Mikado* (Chen et al., 2017) may be helpful for investigating the effect of fibril structures on the mechanical behavior. The current model was limited to 2 dimensions, further extension of the model to include the third dimension will enable the modeling of water and proteoglycan for studying water or proteoglycan-collagen interaction for future applications.

5. Limitations

While the present two-dimensional finite element model provides insight into collagen fibril crosslink-density effects, several simplifying assumptions may affect its quantitative accuracy. First, the model is restricted to 2D geometry and does not capture three-dimensional fibril network interactions or fluid-solid interaction. Second, crosslink patterns were generated via random horizontal node displacement, which may not fully represent the true superficial-zone architecture observed in electron microscopy. Third, fibril and crosslink material properties were fitted from ligament (type I collagen) data due to the lack of direct type II collagen measurements; future work will incorporate experimentally measured viscoelastic parameters for type II collagen fibrils. Fourth, boundary conditions constrain transverse motion, simplifying the multi-axial constraints experienced *in vivo*. Addressing these limitations will require extension to 3D microstructures, direct mechanical testing of type II collagen fibrils, and coupling with proteoglycan and fluid phases.

6. Conclusions

A 2-D finite element model of the collagen fibril network in the superficial zone of the articular cartilage was developed to investigate the effect of the interconnectivity of the structure (crosslink densities) on the time-dependent mechanical responses of the fibrils under cyclic uniformly distributed tensile loads. Increasing the crosslink density increased the resistance to bulk deformation but also increased the local fibril strains and stresses, leading to an increased risk of early fibril failure. Under simulated repetitive loadings, low-density models showed smaller fibril average and peak strains and larger bulk strains than models with higher crosslink densities. This study establishes an initial framework for exploring micro-scale collagen network mechanics and informing future multiscale cartilage models; subsequent work will validate the model against experimental data and extend it to three dimensions. Future developments will aim to incorporate larger-scale architectures and fluid dynamics to more accurately reflect the complex arcade-like collagen organization throughout cartilage.

CRediT authorship contribution statement

Ivan Komala: Writing – original draft, Visualization, Validation, Software, Methodology, Investigation, Formal analysis. **Yu-Ting Chen:** Writing – review & editing, Validation, Software, Methodology, Formal analysis. **Ying-Chun Chen:** Supervision, Methodology, Investigation, Conceptualization. **Chih-Ching Yeh:** Visualization, Validation, Software, Formal analysis. **Tung-Wu Lu:** Writing – review & editing, Supervision, Resources, Project administration, Methodology, Funding acquisition, Data curation, Conceptualization.

Declaration of competing interest

The authors declare that they have no known competing financial interests or personal relationships that could have appeared to influence the work reported in this paper.

Acknowledgment

The authors are grateful for the financial support from the National Science and Technology Council of Taiwan (NSTC 109-2221-E-002 -052 -MY3).

Data availability

Data will be made available on request.

References

Afara, I.O., et al., 2015. Optical absorption spectra of human articular cartilage correlate with biomechanical properties, histological score and biochemical composition. Physiol. Meas. 36 (9), 1913–1928.
Aigner, T., Stöve, J., 2003. Collagens–major component of the physiological cartilage matrix, major target of cartilage degeneration, major tool in cartilage repair. Adv. Drug Deliv. Rev. 55 (12), 1569–1593.
Arokoski, J., et al., 1996. Decreased birefringence of the superficial zone collagen network in the canine knee (stifle) articular cartilage after long distance running training, detected by quantitative polarised light microscopy. Ann. Rheum. Dis. 55 (4), 253–264.
Ateshian, G.A., et al., 2009. Modeling the matrix of articular cartilage using a continuous fiber angular distribution predicts many observed phenomena. J. Biomech. Eng.-Transact. Asme 131 (6).
Athanasiou, K.A., et al., 2013. Articular Cartilage. CRC Press.
Ayyalasomayajula, V., Pierrat, B., Badel, P., 2019. A computational model for understanding the micro-mechanics of collagen fiber network in the tunica adventitia. Biomech. Model. Mechanobiol. 18 (5), 1507–1528.
Benninghoff, A., 1925. Form und Bau der Gelenkknorpel in ihren Beziehungen zur Funktion. Z. Anat. Entwicklungsgeschichte 76 (1–3), 43–63.
Böttcher, P., et al., 2009. Mapping of split-line pattern and cartilage thickness of selected donor and recipient sites for autologous osteochondral transplantation in the canine stifle joint. Vet. Surg. 38 (6), 696–704.
Bridgman, P.W., 2013. Studies in Large Plastic Flow and Fracture: with Special Emphasis on the Effects of Hydrostatic Pressure. Harvard University Press.
Broom, N., Chen, M.H., Hardy, A., 2001a. A degeneration-based hypothesis for interpreting fibrillar changes in the osteoarthritic cartilage matrix. J. Anat. 199 (Pt 6), 683–698.

Broom, N., Chen, M.H., Hardy, A., 2001b. A degeneration-based hypothesis for interpreting fibrillar changes in the osteoarthritic cartilage matrix. J. Anat. 199, 683–698.
Brown, C.P., et al., 2012. Damage initiation and progression in the cartilage surface probed by nonlinear optical microscopy. J. Mech. Behav. Biomed. Mater. 5 (1), 62–70.
Brown, C.P., et al., 2014. Imaging and modeling collagen architecture from the nano to micro scale. Biomed. Opt. Express 5 (1), 233–243.
Buehler, M.J., 2006. Nature designs tough collagen: explaining the nanostructure of collagen fibrils. Proc. Natl. Acad. Sci. 103 (33), 12285–12290.
Bullough, P., Goodfellow, J., 1968. The significance of the fine structure of articular cartilage. J. Bone Joint Surg. Br 50 (4), 852–857.
Burstein, D., Gray, M.L., 2006. Is MRI fulfilling its promise for molecular imaging of cartilage in arthritis? Osteoarthr. Cartil. 14 (11), 1087–1090.
Casey, D.T., et al., 2021. Percolation of collagen stress in a random network model of the alveolar wall. Sci. Rep. 11 (1), 16654.
Chen, M.H., Broom, N., 1998a. On the ultrastructure of softened cartilage: a possible model for structural transformation. J. Anat. 192 (Pt 3), 329–341.
Chen, M.H., Broom, N., 1998b. On the ultrastructure of softened cartilage: a possible model for structural transformation. J. Anat. 192, 329–341 (Pt 3)(Pt 3).
Chen, Y.C., et al., 2017. Effect of crosslinking in cartilage-like collagen microstructures. J. Mech. Behav. Biomed. Mater. 66, 138–143.
Chen, Y.C., Brown, C.P., 2020. Embrittlement of collagen in early-stage human osteoarthritis. J. Mech. Behav. Biomed. Mater. 104.
Cook, T.M., et al., 1997. Effects of restricted knee flexion and walking speed on the vertical ground reaction force during gait. J. Orthop. Sports Phys. Ther. 25 (4), 236–244.
Dahaghin, S., et al., 2009. Squatting, sitting on the floor, or cycling: are life-long daily activities risk factors for clinical knee osteoarthritis? Stage III results of a community-based study. Arthritis Rheum. 61 (10), 1337–1342.
de Andréa Dernowsek, J., et al., 2019. Micro finite element analysis of hierarchical layers of the articular cartilage for biofabrication. J. Mech. Eng. Biomech. 3 (5), 7.
Deneweth, J.M., McLean, S.G., Arruda, E.M., 2013. Evaluation of hyperelastic models for the non-linear and non-uniform high strain-rate mechanics of tibial cartilage. J. Biomech. 46 (10), 1604–1610.
Depalle, B., et al., 2015. Influence of cross-link structure, density and mechanical properties in the mesoscale deformation mechanisms of collagen fibrils. J. Mech. Behav. Biomed. Mater. 52, 1–13.
Eyre, D., 2001. Articular cartilage and changes in arthritis: collagen of articular cartilage. Arthritis Res. Ther. 4 (1), 30.
Glover, P., Mansfield, S.P., 2002. Limits to magnetic resonance microscopy. Rep. Prog. Phys. 65 (10), 1489–1511.
Goodwin, D.W., et al., 2004. Macroscopic structure of articular cartilage of the tibial Plateau: influence of a characteristic matrix architecture on MRI appearance. Am. J. Roentgenol. 182 (2), 311–318.
Guilak, F., et al., 1994. Mechanical and biochemical changes in the superficial zone of articular cartilage in canine experimental osteoarthritis. J. Orthop. Res. 12 (4), 474–484.
Heidari, B., 2011. Knee osteoarthritis prevalence, risk factors, pathogenesis and features: part I. Caspian J. Intern Med. 2 (2), 205–212.
Huber, M., Trattnig, S., Lintner, F., 2000. Anatomy, biochemistry, and physiology of articular cartilage. Investig. Radiol. 35 (10), 573–580.
Hwang, W., et al., 1992. Collagen fibril structure of normal, aging, and osteoarthritic cartilage. J. Pathol. 167 (4), 425–433.
Johansson, A., et al., 2011. A spectroscopic approach to imaging and quantification of cartilage lesions in human knee joints. Phys. Med. Biol. 56 (6), 1865–1878.
Julkunen, P., et al., 2007. Characterization of articular cartilage by combining microscopic analysis with a fibril-reinforced finite-element model. J. Biomech. 40 (8), 1862–1870.
Korhonen, R., et al., 2002. Importance of the superficial tissue layer for the indentation stiffness of articular cartilage. Med. Eng. Phys. 24 (2), 99–108.
Lai, W.M., Hou, J., Mow, V.C., 1991. A Triphasic Theory for the Swelling and Deformation Behaviors of Articular Cartilage.
Leo, B.M., Turner, M.A., Diduch, D.R., 2004. Split-line pattern and histologic analysis of a human osteochondral plug graft. Arthroscopy 20 (Suppl. 2), 39–45.
Li, X., et al., 2007. <Em>In vivo T$_{1\rho}$ and T$_2$ mapping of articular cartilage in osteoarthritis of the knee using 3T MRI. Osteoarthr. Cartil. 15 (7), 789–797.
Li, Y., et al., 2019. Decellularized cartilage matrix scaffolds with laser-machined micropores for cartilage regeneration and articular cartilage repair. Mater. Sci. Eng. C 105, 110139.
Liu, J., et al., 2018. Energy dissipation in Mammalian collagen fibrils: cyclic strain-induced damping, toughening, and strengthening. Acta Biomater. 80, 217–227.
Loening, A.M., et al., 2000. Injurious mechanical compression of bovine articular cartilage induces chondrocyte apoptosis. Arch. Biochem. Biophys. 381 (2), 205–212.
Mononen, M.E., et al., 2012. Effect of superficial collagen patterns and fibrillation of femoral articular cartilage on knee joint mechanics-A 3D finite element analysis. J. Biomech. 45 (3), 579–587.
Mow, V., et al., 1984. Viscoelastic properties of proteoglycan subunits and aggregates in varying solution concentrations. J. Biomech. 17 (5), 325–338.
Mündermann, A., Dyrby, C.O., Andriacchi, T.P., 2005. Secondary gait changes in patients with medial compartment knee osteoarthritis: increased load at the ankle, knee, and hip during walking. Arthritis Rheum. 52 (9), 2835–2844.
Oberg, P.A., Sundqvist, T., Johansson, A., 2004. Assessment of cartilage thickness utilising reflectance spectroscopy. Med. Biol. Eng. Comput. 42 (1), 3–8.
Ogden, R.W., 1997. Non-linear elastic deformations. Courier Corporation.
Orford, C.R., Gardner, D.L., Oconnor, P., 1983. Ultrastructural-changes in dog femoral condylar cartilage following anterior cruciate ligament section. J. Anat. 137 (Dec), 653–663.
Panula, H.E., et al., 1998. Articular cartilage superficial zone collagen birefringence reduced and cartilage thickness increased before surface fibrillation in experimental osteoarthritis. Ann. Rheum. Dis. 57 (4), 237–245.
Pierce, D.M., et al., 2009. A phenomenological approach toward patient-specific computational modeling of articular cartilage including collagen fiber tracking. J. Biomech. Eng.-Transact. Asme 131 (9).
Pierce, D.M., Ricken, T., Holzapfel, G.A., 2013. A hyperelastic biphasic fibre-reinforced model of articular cartilage considering distributed collagen fibre orientations: continuum basis, computational aspects and applications. Comput. Methods Biomech. Biomed. Eng. 16 (12), 1344–1361.
Radin, E.L., et al., 1984. Effects of mechanical loading on the tissues of the rabbit knee. J. Orthop. Res. 2 (3), 221–234.
Saarakkala, S., et al., 2010. Depth-wise progression of osteoarthritis in human articular cartilage: investigation of composition, structure and biomechanics. Osteoarthr. Cartil. 18 (1), 73–81.
Shirazi, R., Shirazi-Adl, A., Hurtig, M., 2008. Role of cartilage collagen fibrils networks in knee joint biomechanics under compression. J. Biomech. 41 (16), 3340–3348.
Stein, A.M., et al., 2008. An algorithm for extracting the network geometry of three-dimensional collagen gels. J. Microsc. 232 (3), 463–475.
Susilo, M.E., et al., 2016a. Collagen network strengthening following cyclic tensile loading. Interface Focus 6 (1), 20150088.
Susilo, M.E., et al., 2016b. Collagen network strengthening following cyclic tensile loading, 6 (1), 20150088.
Tang, Y., et al., 2010. Deformation micromechanisms of collagen fibrils under uniaxial tension. J. Royal Soc. 7 (46), 839–850. Interface.
Tang, B., et al., 2014. Nanostiffness of collagen fibrils extracted from osteoarthritic cartilage characterized with AFM nanoindentation. Soft Mater. 12 (3), 253–261.
Teshima, R., et al., 1995. Structure of the Most superficial layer of articular-cartilage. J. Bone Jt. Surg. Br. Vol. 77b (3), 460–464.
Thambyah, A., Broom, N., 2006. Micro-anatomical response of cartilage-on-bone to compression: mechanisms of deformation within and beyond the directly loaded matrix. J. Anat. 209 (5), 611–622.
van der Rijt, J.A.J., et al., 2006. Micromechanical testing of individual collagen fibrils. Macromol. Biosci. 6 (9), 697–702.
Verzijl, N., et al., 2002. Crosslinking by advanced glycation end products increases the stiffness of the collagen network in human articular cartilage - a possible mechanism through which age is a risk factor for osteoarthritis. Arthritis Rheum. 46 (1), 114–123.
Wang, J.-Y., et al., 2021a. Micro-mechanical damage of needle puncture on Bovine annulus fibrosus fibrils studied using polarization-resolved second harmonic generation (P-SHG) microscopy. J. Mech. Behav. Biomed. Mater. 118, 104458.
Wang, Y., Sun, S., 2021b. Multiscale pore structure characterization based on SEM images. Fuel 289, 119915.
Wilson, W., et al., 2004. Stresses in the local collagen network of articular cartilage: a poroviscoelastic fibril-reinforced finite element study. J. Biomech. 37 (3), 357–366.
Woo, S.L.Y., et al., 2006. Biomechanics of knee ligaments: injury, healing, and repair. J. Biomech. 39 (1), 1–20.
Yang, L., et al., 2012. Micromechanical analysis of native and cross-linked collagen type I fibrils supports the existence of microfibrils. J. Mech. Behav. Biomed. Mater. 6, 148–158.
Zhao, W., et al., 2020. Synthetic/Natural blended polymer fibrous meshes composed of polylactide, gelatin and glycosaminoglycan for cartilage repair. J. Biomater. Sci. Polym. Ed. 31 (11), 1437–1456.